A THERMO-FLUID MODEL FOR PROTECTIVE SUITING USED IN FUSION REACTOR SHUTDOWN OPERATIONS

K. Tesch[a], M.W. Collins[b], T.G. Karayiannis[b], M.A. Atherton[b], P. Edwards[c]

[a] *Gdansk University of Technology, Fluid Mechanics Dept., ul. G. Narutowicza 11/12, 80-952 Gdansk, Poland*
[b] *Brunel University, School of Engineering and Design,West London, Uxbridge, Middlesex UB8 3PH, U.K.*
[c] *UKAEA Culham Division, Culham Science Centre, Abingdon, Oxfordshire OX14 3DB, U.K.*

ABSTRACT

In this paper we report a method of modelling the overall thermo-fluid processes which occur in protective suiting as used in the Joint European Torus (JET) fusion reactor at Culham, UK. It had three main objectives: to be as basic and comprehensive as possible, to have an ability to model real situations and suiting, and hence to provide a tool for improvements in design. Basic thermo-fluids equations for multi-component and multi-phase flow have been developed within commercial Computational Fluid Dynamics (CFD) software to address the heat and mass (moisture) transfer processes. This is combined with a human metabolic heat load model to simulate working operations. Finally, a particular feature is the definition of the 3-D human body/suit microclimate, via the use of an unsuited and suited mannequin. This involved a geometrical reconstruction method developed from the point cloud data given by photogrammetry. Examples of predicted temperature distributions are compared with experimental data to show the potential of the model we have used..

BACKGROUND

The Culham Science Centre, near Oxford, UK, hosts the JET reactor whose programme is integrated with the future ITER under construction at Cadarache, France. The reactor undergoes periodical shutdown periods for maintenance and enhancement connected with the exploitation programme.

Workers carrying out these activities wear pressurised suiting, which protects against both inhalation and contamination of tritium and beryllium.

The design of the suit has developed empirically, and this is inadequate for two reasons. Firstly, there is the practical necessity of ensuring the design is optimal for worker performance and thermal comfort. Secondly, engineering substantiation may be a further requirement.

These reasons provide the rationale for developing a comprehensive thermo-fluid model of the system, and especially of the microclimate between the worker and the internal surface of the suit fabrics. Moreover, a comprehensive model should provide generic information, relating to design of similar suiting used in the nuclear fission and chemical industries and some defence (military) applications.

FLOW DOMAIN

A life-sized marching mannequin was loaned by Defence Science and Technology Laboratory (dstl) at Porton Down, UK to the UK Atomic Energy Authority (UKAEA) Culham, the management organisatrion for JET. An experiment was conducted by UKAEA in which the mannequin was firstly used in an unsuited mode and secondly fitted with a real pressurised suit in a variety of working positions.

Sets of scanned data were obtained by means of photogrammetry, which is a remote sensing technology in which geometric properties of objects are determined from photographic images. Many photographs of the object are taken from different angles allowing common points to be identified on each image. A line of sight can then be constructed from the camera location to a point on the object. It is the intersection of these rays that determines the three-dimensional location of the point. UKAEA use photogrammetry as part of its daily procedures to measure critical components that are difficult to measure by conventional methods. The equipment currently used allows an accuracy of ±10 microns.

Fig. 1. Real mannequin in a suit

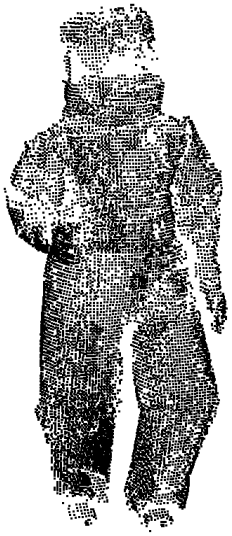

Fig.2. Point cloud

The suited mannequin is shown in fig.1. Output from the photogrammetry is in the form of point cloud data, a typical set of which is shown in fig.2. From the point cloud data it is necessary to reconstruct 3-D surfaces for both mannequin and suit, to be directly input as geometrical boundaries for the CFD calculations. The reconstruction process must be of high accuracy, as the microclimate for thermofluids calculations is defined by the separation beween the two surfaces. This necessitated the use of a time-intensive manual method. Figure 3 shows a typical set of reconstructed geometries, corresponding to the point clouds of fig 2 and the previous unsuited mannequin test. The reconstruction of fig. 3 is in a sufficiently compatible form for the CFD preprocessor software to mesh.

Finally, it should be borne in mind that our double scanning method involved exact positional correspondence of the unsuited and suited mannequin modes. It would be very difficult to achieve the required accuracy using the alternative of a real human subject.

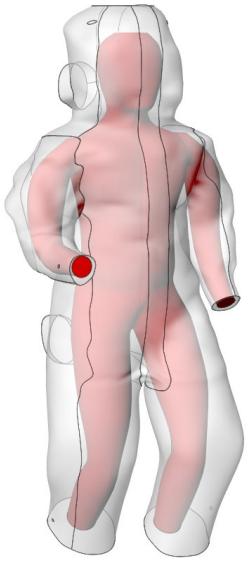

Fig.3. Reconstructed geometry of a suit and a mannequin

THERMO-FLUIDS MODEL

Two-component turbulent flow

The flow of air within the air gap is turbulent and two-component due to the presence of water vapour in the air. The vapour appears in the air, as originally supplied by umbilical feed, by way of the respiration process and moisture produced by the human body. A two-component model, therefore, is likely to predict the flow more accurately.

For a multi-component flow a common assumption is that all the variables except concentration share the same fields. Most of the equations for single-phase and single-component flows have exactly the same form. The time-averaged form of mass conservation

$$\frac{\partial \bar{U}_i}{\partial x_i}. \tag{1}$$

The Reynolds equation is

$$\frac{\partial\left(\rho\bar{U}_j\right)}{\partial t}+\frac{\partial\left(\rho\bar{U}_i\bar{U}_j\right)}{\partial x_i}=\rho\bar{f}_j-\frac{\partial p_e}{\partial x_j}+\frac{\partial\left(2\mu_e\bar{D}_{ij}\right)}{\partial x_i} \tag{2}$$

where the effective viscosity $\mu_e := \mu+\mu_t$ and effective pressure $p_e := p+2/3\rho k$. The eddy viscosity concept is used with the Reynolds stress tensor described by means of the Boussinesq hypothesis.

The two equation standard $k-\varepsilon$ turbulence model is adopted here. The first transport equation is for the kinetic energy k of velocity fluctuations, and comes from the Reynolds stress transport equation as

$$\begin{aligned}&\frac{\partial(\rho k)}{\partial t}+\frac{\partial\left(\rho k\bar{U}_i\right)}{\partial x_i}=2\mu_t\bar{D}_{ij}\bar{D}_{ij}\\&+\frac{\partial}{\partial x_i}\left(\left(\frac{\mu_t}{\sigma_k}+\mu\right)\frac{\partial k}{\partial x_i}\right)-\rho\varepsilon\end{aligned} \tag{3}$$

The second is for the dissipation ε of the kinetic energy, and is analogous in form to that for k, namely

$$\begin{aligned}&\frac{\partial(\rho\varepsilon)}{\partial t}+\frac{\partial\left(\rho\varepsilon\bar{U}_i\right)}{\partial x_i}=C_{\varepsilon1}\frac{\varepsilon}{k}2\mu_t\bar{D}_{ij}\bar{D}_{ij}\\&+\frac{\partial}{\partial x_i}\left(\left(\frac{\mu_t}{\sigma_\varepsilon}+\mu\right)\frac{\partial\varepsilon}{\partial x_i}\right)-C_{\varepsilon2}\rho\frac{\varepsilon^2}{k}\end{aligned} \tag{4}$$

The eddy viscosity μ_t depends on both k and ε and is postulated to have the form

$$\mu_t=C_\mu\rho\frac{k^2}{\varepsilon} \tag{5}$$

The five constants in the above equations are empirical (that is deduced from experiment for a specific geometry) and the 'standard' set [5] is given by $\sigma_k=1$, $\sigma_\varepsilon=1.3$, $C_\mu=0.09$, $C_{\varepsilon1}=1.44$, $C_{\varepsilon2}=1.92$.

Mass and heat transfer

The time-averaged concentration transport equation may be written as

$$\frac{\partial\left(\rho\overline{g}^{\alpha}\right)}{\partial t}+\frac{\partial\left(\rho\overline{g}^{\alpha}\overline{U}_i\right)}{\partial x_i}=\frac{\partial}{\partial x_i}\left(\rho D_e\frac{\partial\overline{g}^{\alpha}}{\partial x_i}\right) \tag{6}$$

using the eddy diffusivity operator D_e. It is represented as a function of the eddy viscosity and the turbulent Schmidt number Sc_t, namely as $D_e \coloneqq \mu_t\rho^{-1}\mathrm{Sc}_t^{-1}+D^{\alpha\beta}$.

The time-averaged Fourier-Kirchhoff (inner energy) equation for a two-component flow differs from that for a single-component flow, because of an additional term responsible for the diffusion of internal energy

$$c_v\left(\frac{\partial\left(\rho\overline{T}\right)}{\partial t}+\frac{\partial\left(\rho\overline{T}\overline{U}_i\right)}{\partial x_i}\right)=2\mu\overline{D}_{ij}\overline{D}_{ij}$$
$$+\frac{\partial}{\partial x_i}\left(\lambda_e\frac{\partial\overline{T}}{\partial x_i}+\rho\overline{T}\sum_{i=1}^{2}c_v^{\alpha}D^{\alpha\beta}\frac{\partial\overline{g}^{\alpha}}{\partial x_i}\right)+\rho\varepsilon. \tag{7}$$

Here the effective conductivity λ_e arises from the eddy diffusivity hypothesis. It is obtained, using the turbulent Prandtl number Pr_t, as $\lambda_e \coloneqq \mu_t c_v\,\mathrm{Pr}_t^{-1}+\lambda$. We assume that the correlation of the temperature and the concentration fluctuation are neglected.

More detailed discussion about the relationship of these multi-component and multi-phase equations may be found in [2].

The closed system of equations

There are eight unknown functions $\overline{U}_i$, $\overline{p}$, k, ε, μ_t, $\overline{T}$, $\overline{g}^1$, $\overline{g}^2$ and seven scalar equations (1)-(7) which means that one additional equation has to be added to close the system. There is no need to involve an additional transport equation for concentration $\overline{g}^2$ because the so called constraint equation

$$\overline{g}^2=1-\overline{g}^1 \tag{8}$$

may be used. This is algebraic, whereas the equation of transport of concentration is differential.

Boundary conditions

To solve the closed system the correct boundary conditions must be formulated.

The suit shown in figure (1) has six inlets: two each above the head, near the wrists and near the ankles. At these locations it is necessary to specify the volumetric flow rate, temperature, the turbulence intensity $\overline{U}^{-1}\sqrt{2/3k}$ and the viscosity ratio μ_t/μ.

The suit has four outlets, two each above the head and at the lower part of the back. A constant static pressure is specified.

All velocity components at the wall are zero. The bulk heat flux (there are also other alternatives) is specified by means of a combined heat transfer coefficient h and the ambient temperature T_a as $q_n=h\left(T-T_a\right)$. For the suit (outer) boundary condition the ambient temperature is taken as the torus temperature. For the body surface (inner) boundary condition the core body temperature T_b is taken. This temperature depends on a number of variables including the metabolic rate MW, the environment and the clothing. A simple method of calculating T_b and its rate of change was applied here based on a metabolic heat balance [4]. This makes it possible to predict the processes that affect it. T_b is normally about 310 K resulting from the balance between the amount of heat produced by the body and losses due to a number of different phenomena.

EXAMPLE OF RESULTS FOR A TYPICAL WORKING OPERATION

Experiments were performed at JET [2] and results for a typical operation are shown in fig. 4. The variations in conditions with time over a 90 minute regime are summarised by metabolic rate MW and production of vapour m_v. The initial period (36 minutes) represents a stabilisation of conditions. During this time no physical activity took place. From 36 to 49 min. the worker had a moderate output due only to walking. This was followed by a period from 49 to 68 min. of hard (working) activity. The final period from 68 to 82 min. corresponds to cooling without any physical activity.

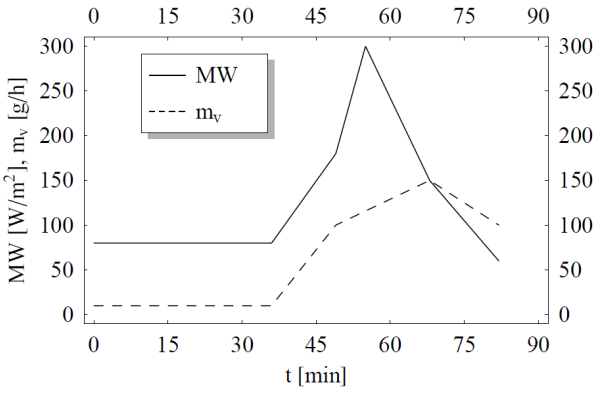

Fig.4. Metabolic heat load and vapour production [2]

The time-dependent physical load causes the body temperature to vary from its equilibrium level of 310 K as shown in figure fig.5. The core temperature stays nearly constant until the person begins to perform work, then rises consistently until a slight decrease takes place after the physical activity is stopped.

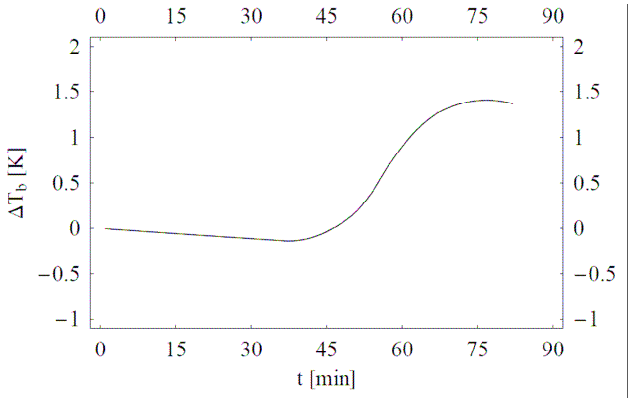

Fig. 5 Body temperature variation

Figure 6 shows a comparison of numerical predictions of outlet temperature using the $k-\varepsilon$ turbulence model with measurements. The overall model and bulk heat transfer assumptions are evidently sufficiently satisfactory to predict the temperature variations caused by human body metabolic activity.

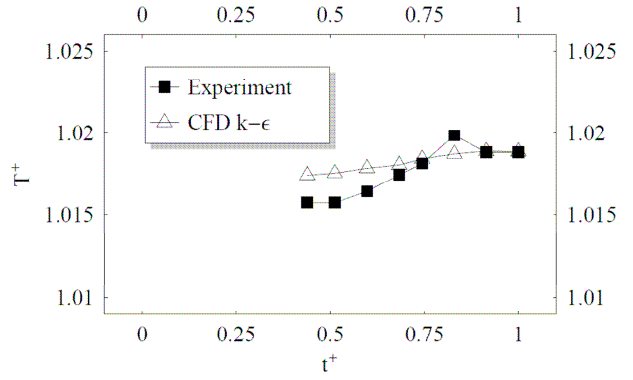

Fig. 6. Comparison of numerical predictions with measurements of the outlet temperature

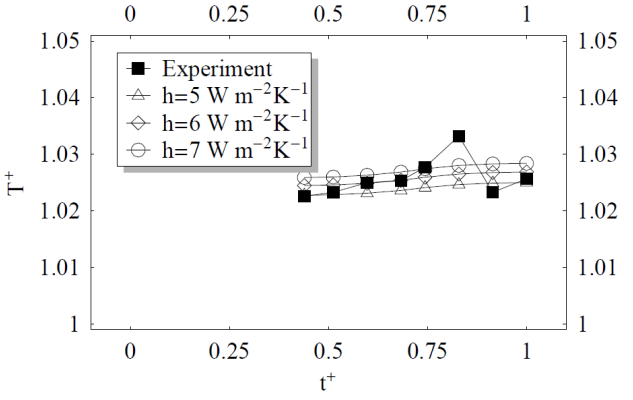

Fig. 7. Comparison of numerical predictions with measurements of the upper arm temperature

Satisfactory agreement of the numerical predictions and measurements may also be seen for the upper arm and torso temperatures in figures 7 and 8 respectively. These figures also show how the predictions depend on the body side heat transfer coefficient h. The results indicate that non-constant values of h would better fit the experimental data. However, to include such a variation would require further experimental investigation.

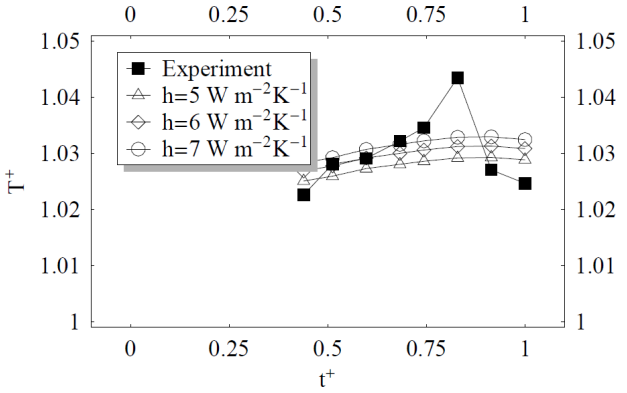

Fig. 8. Comparison of numerical predictions with measurements of the upper torso temperature

The above measurements took place at time steps of 36, 42, 49, 56, 61, 68, 75 and 82 min.

Predictions of the temperature distributions for skin and suit at these times are shown in figures 9 and 10 respectively. Of course, here the real human suited subject has been modelled by the reconstructed geometry of the suited mannequin. The variations in these distributions are caused by the changes in metabolic heat load. The distributions are asymmetric because of the asymmetric mannequin position as shown in fig. 3. The presence of hot spots may be the reason for the known occurrences of thermal discomfort suffered by the workers. A comparison of distributions in fig. 10 with those corresponding to them in fig. 9, shows that variations in the suit temperature are negligible.

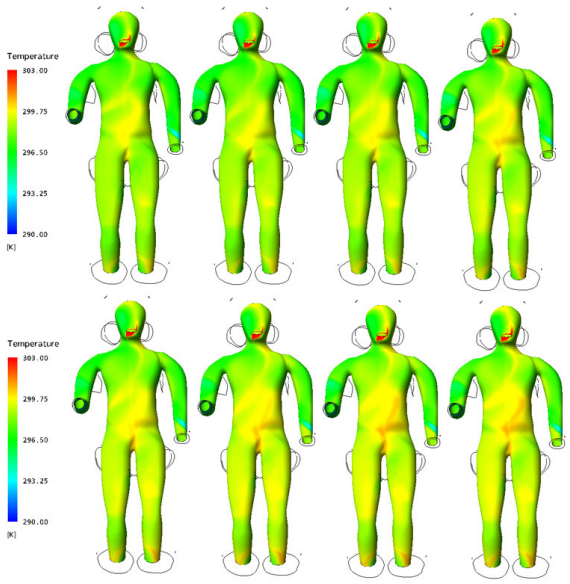

Fig. 9 Body temperature at time step 36, 42, 49, 56, 61, 68, 75 and 82 min.

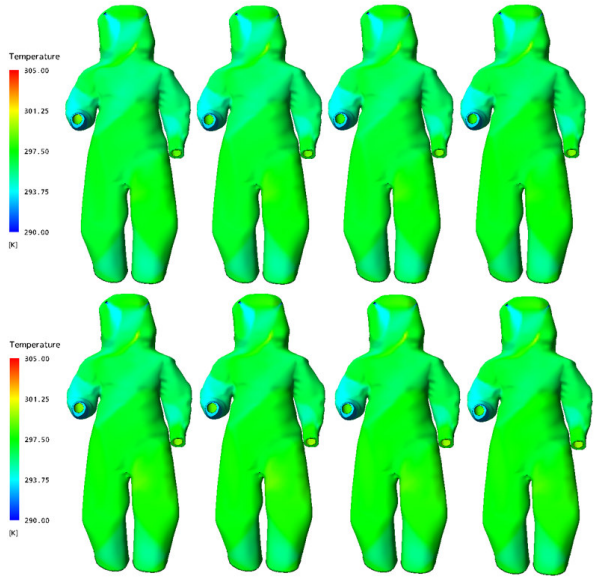

Fg:10. Suit temperature at time step 36, 42, 49, 56, 61, 68, 75 and 82 min.

CONCLUSIONS

The thermofluid processes in the microclimate of fully pressurised suits used during fusion reactor shut-down periods have been comprehensively modelled. The model is composed of a CFD core, together with: additional equations for moisture transport, a pre-processor data input facility accommodating a geometry reconstructed from the scanning of a suited mannequin, and a whole-body human metabolic heat load model. The overall model has been successfully used in predictive mode, and compared with results of matching experiments. Current work includes investigating the effects of modifying the suit design in order to try to eliminate the presence of hot spots on the skin surface. We hope to extend the model further by incorporating consideration of multi-layer suiting fabric and more general human metabolic modelling.

NOMENCLATURE

Symbol	Quantity	SI Unit
c_v , c_v^{α}	specific heat capacity	$\mathrm{J\,kg^{-1}K^{-1}}$
$C_{\varepsilon 1}$, $C_{\varepsilon 2}$, C_{μ}	$k-\varepsilon$ turbulence model constants	
$\bar{D}_{ij}$	average strain rate tensor	$\mathrm{s^{-1}}$
D_e	effective diffusivity	$\mathrm{m^2 s^{-1}}$
$D^{\alpha\beta}$	diffusivity coefficient	$\mathrm{m^2 s^{-1}}$
$\bar{f}_i$	external force	$\mathrm{kg\,m^{-2}s^{-2}}$
g^{α}	concentration	
h	heat transfer coefficient	$\mathrm{W\,m^2K^{-1}}$
k	kinetic energy of velocity fluctuations	$\mathrm{m^2 s^{-2}}$
MW	metabolic rate	$\mathrm{W\,m^{-2}}$
$\bar{p}$, p_e	average and effective pressure	Pa
Pr_t	turbulent Prandtl number	
q_n	bulk heat flux	$\mathrm{W\,m^{-2}}$
Sc_t	turbulent Schmidt number	
t , t^+	time and dimensionless time	s ,-
$\bar{T}$, T_a , T_b , T^+	average, ambient, body and dimensionless temperatures	K ,-
$\bar{U}^i$	average velocity component	$\mathrm{m\,s^{-1}}$
$\bar{U}$	velocity magnification	$\mathrm{m\,s^{-1}}$
x_i	axes	m
α	component	
ε	dissipation of fluctuation of kinetic energy	$\mathrm{W\,kg}$
λ , λ_e	conductivity and effective conductivity	$\mathrm{W\,m^{-1}K^{-1}}$
μ , μ_e , μ_t	molecular, effective and eddy viscosity	$\mathrm{kg\,m^{-1}s^{-1}}$
ρ	density	$\mathrm{kg\,m^{-3}}$
σ_k , σ_{ε}	$k-\varepsilon$ turbulence model constants	

REFERENCES

[1] M. Ishii and T. Hibiki, Thermo-Fluid Dynamics of Two-Phase Flow, Springer, 2006.

[2] K. Tesch, T.G. Karayiannis, M.W. Collins, M.A. Atherton and P. Edwards, Heat and Mass Transfer in Air-Fed Pressurised Suits, *Proc. UK Heat Transfer Conference, Edinburgh 2007*

[3] K. Tesch, T.G. Karayiannis, M.W. Collins, M.A. Atherton and P. Edwards, Heat Transfer Coefficient Calibrations by Means of Evolutionary Algorithms, *Proc. Adaptive Computing in Design and Manufacture, Bristol U.K., 2008*

[4] K. Tesch, T.G. Karayiannis, M.W. Collins, M.A. Atherton and P. Edwards, Thermo-fluid Transport Phenomena in Air-fed Pressurised Protective Clothing, *Proc. HEAT 2008, 5th International Conference on Transport Phenomena in Multiphase Systems, Bialystok, Poland, 2008*

[5] D.C. Wilcox, Turbulence Modeling for CFD, DCW Industries, 1994